A COMPREHENSIVE MODEL OF BIOMASS CARBONIZATION

W. Klose and A.-P. Schinkel
University of Kassel, Institute of Thermal Engineering
Kurt-Wolters-Str. 3, D-34109 Kassel, Germany

Introduction

The pyrolysis process of biomass has been investigated in the frame of adsorbent production and partly fuel substitution. The aim of this investigation is an upgrading of biomass to an easy handling and high calorific fuel. By the pyrolysis process biomass is refined to solid fuels or precursors for the adsorbent production. The yields and properties of this process are strongly related to the process conditions. Therefore a mathematical model for the pyrolysis process using a rotary kiln has been formulated. One of the major parameters, the residence time of the solids, has been investigated in detail. A lot of analytical and empirical formulas have been developed concerning the flow patterns rolling and slipping. The deviations of the analytical derived equations from the measurements lead to a large number of empirical equations. One reason for these deviations is a flow pattern that combines two kinds of motion. This discovered flow type will be discussed in detail.

Granular Flow Patterns

For rotary kiln processes usually four basic flow pattern, shown in figure 3, can be distinguished: slipping, slumping, rolling, and cascading. Slipping occurs for low filling ratios of the tube. The granular material slips at the wall of the tube. No shear rate can be observed in the granular material. The motion of steady-state sliding is modeled by Heiligenstaedt [1]. This equation describes the motion along a screwline on the reactor wall. For higher filling ratios the flow pattern changes to slumping, rolling, or cascading. The granular material slumps discontinuously down at the free surface during the slumping bed motion. For higher rotational speed this flow pattern turns over to a continuously motion at the free surface. This flow pattern is called rolling if the granular bed is in the lower half of the tube. If it is partly in the upper half this continuously bed motion is called cascading. These flow patterns can be described by the equation of Saeman [3]. In figure 1 a bed behaviour diagram, suggested by Henein [2], is shown for maize for different values of slipping friction. For non horizontal

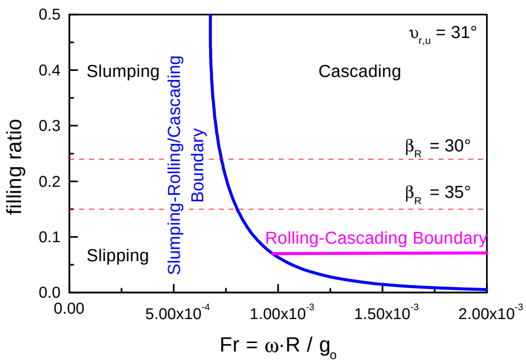

Figure 1: Bed behaviour diagram of maize

drums the filling ratio decreases continuously from the reactor inlet to a vanishing value at the outlet. Therefore, the bed motion can change from rolling, cascading, or slumping to a kind of slipping motion. If the volume flux of the rolling transport is greater than the possible volume flux of the slipping transport a mixture of slipping and slumping occurs. The deviation of measurements from the equations describing the pure flow patterns is shown in figure 2. The discontinuous slipping of the bed is stabilized by the slumping part of the bed motion, it can not be described by the model of Heiligenstaedt. An additional flow model for this kind of discontinuous slipping transport will be discussed.

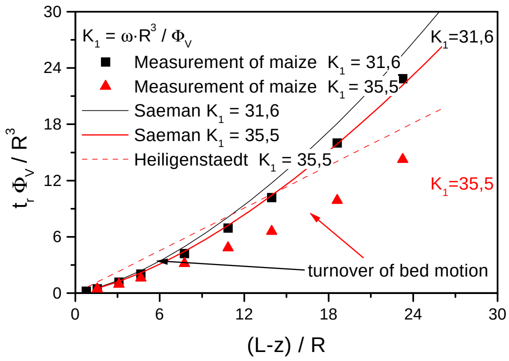

Figure 2: Measurements and model results of the residence time t_r of maize along the axial coordinate

Discontinuous Slipping Model

The granular material is lifted by the reactor wall up to the upper angle of slipping friction. At this point the bed begins to slide a bit upwards, then downwards, the direction of slipping changes again, and the slipping motion stops if the angular velocity of the bed is equivalent to the kiln's one. During the slipping phase an axial transport of the bed can be observed due to the slope of the kiln. The balance of the angular momentum of the granular bed is expressed as

$$J_r \cdot \frac{d^2\upsilon}{dt^2} = -F_G \cdot r_s \cdot \cos\kappa \cdot \sin\upsilon + F_{R,Q} \cdot R. \quad (1)$$

The gravity force is denoted by F_G, the friction force by $F_{R,Q}$, the radius of the center of mass of the granular bed by r_s , the kiln radius by R, and the incline of the kiln by κ. The moment of inertia J_r for the granular bed concerning the tube axis J_r is written as

$$J_r = 2 \cdot \rho \cdot L \cdot \int_{r_o}^{R} r^2 \cdot \sqrt{R^2 - r^2} dr \quad (2)$$

$$= \frac{1}{4} \cdot \rho \cdot L \cdot \left[\frac{\pi}{2} \cdot R^4 + 2 \cdot r_o \left(R^2 - r_o^2\right)^{3/2} \right. \quad (3)$$

$$\left. - R^2 \cdot r_o \sqrt{R^2 - r_o^2} - R^4 \arctan\left(\frac{r_o}{\sqrt{R^2 - r_o^2}} \right) \right]. \quad (4)$$

Where $r_o$is the surface radius. The balance of the angular momentum leads to

$$J_r \cdot \frac{d^2\upsilon}{dt^2} = -F_G \cdot \cos\kappa \cdot r_s \cdot \sin\upsilon + F_G \cdot \cos\kappa \cdot \sqrt{1 - \left(\frac{r_s \cdot \sin\upsilon}{R}\right)^2} \cdot \tan\beta_R \cdot \frac{R \cdot \left|\frac{d\upsilon}{dt}\right|}{\sqrt{\left(R \cdot \frac{d\upsilon}{dt}\right)^2 + \left(\frac{dz}{dt}\right)^2}} \cdot R. \quad (5)$$

In this equation the lower bed-wall friction angle is denoted by β_R.The momentum balance for the axial direction (z) leads to

$$m \cdot \frac{d^2 z}{dt^2} = F_G \cdot \sin\kappa - F_G \cdot \cos\kappa \cdot \sqrt{1 - \left(\frac{r_s \cdot \sin\upsilon}{R}\right)^2} \cdot \tan\beta_R \cdot \frac{\frac{dz}{dt}}{\sqrt{\left(R \cdot \frac{d\upsilon}{dt}\right)^2 + \left(\frac{dz}{dt}\right)^2}}. \quad (6)$$

These two differential equations are solved simultaneously taking the boundary conditions into account

$$\frac{d\upsilon}{dt}\Big|_{\upsilon=\arcsin\frac{R\cdot\sin\beta_{Q,h}}{rs}} = \omega \quad \text{and}$$
$$w\frac{d\,z}{d\,t}\Big|_{\upsilon=\arcsin\frac{R\cdot\sin\beta_{Q,h}}{rs}} = 0. \quad (7)$$

Where the angular velocity of the kiln is expressed by ω. The projection of the upper bed-wall friction angle to the transverse plane of the tube is symbolized by $\beta_{Q,h}$. For inclines of practical rotary kilns (κ =1° − 4°) the momentum balance concerning the tube axis is solved decoupled by neglecting the axial velocity in comparison to the velocity in the transverse plane of the tube. The angular velocity is expressed as

$$\frac{d\upsilon}{dt} = \pm\sqrt{\frac{F_G}{J_r} \cdot \cos\kappa \cdot R \cdot A + \omega^2} \quad (8)$$

with

$$A = \frac{r_s}{R} \cdot (\cos\upsilon - \cos\upsilon_s) + \tan\beta_R \cdot \left[E\left(\upsilon \backslash \arcsin\sqrt{\frac{r_s}{R}}\right) - E\left(\upsilon_s \backslash \arcsin\sqrt{\frac{r_s}{R}}\right)\right]. \quad (9)$$

The incline of the bed in the transverse plane of the tube at the slipping start is denoted by υ_s. The elliptic integral of the second kind is expressed approximately by

$$E(\upsilon \setminus \alpha) \approx (\upsilon - \sin\upsilon) \cdot \cos^2\alpha + \sin\upsilon. \quad (10)$$

The momentum balance in the axial direction is transformed by neglecting the axial velocity in the sum of the second term in eq. (5) to

$$\frac{d^2z}{d\upsilon^2} = \frac{g_0 \cdot \sin\kappa}{\left(\frac{d\upsilon}{dt}\right)^2} - \frac{dz}{d\upsilon}\left(g_0 \cdot \cos\kappa \cdot \sqrt{1 - \left(\frac{r_s \cdot \sin\upsilon}{R}\right)^2} \cdot \frac{\tan\beta_R}{R \cdot \left(\frac{d\upsilon}{dt}\right)^2} + \frac{d\frac{d\upsilon}{dt}}{d\upsilon} \cdot \frac{1}{\frac{d\upsilon}{dt}}\right). \quad (11)$$

Numerical solutions of the differential equations show an approximately linear behaviour of the slipping curve. Therefore, the curvature is neglected. It is convenient to solve this equation at $\upsilon = \arcsin\frac{R \cdot \sin\beta_R}{rs}$ because the term $\frac{d\frac{d\upsilon}{dt}}{d\upsilon}$ is vanishing at this location. The derivative $\frac{dz}{d\upsilon}$ is expressed as

$$\frac{dz}{d\upsilon}\Big|_{\upsilon=\arcsin\frac{R\cdot\sin\beta_R}{rs}} = R \cdot \frac{\tan\kappa}{\sin\beta_R}. \quad (12)$$

The total slipping angle $\Delta\upsilon$, the angle of end of slipping υ_{end} and the slipping time t_{slipp} is calculated from eq. (8). Hence, the velocity for the discontinuously slipping is expressed as

$$w_{d,slipp} = \frac{\frac{dz}{d\upsilon}\Big|_{\upsilon=\arcsin\frac{R\cdot\sin\beta_Q}{rs}} \cdot \Delta\upsilon}{\frac{\arcsin\frac{R\cdot\sin\beta_{Q,h}}{rs} - \upsilon_{end}}{\omega} + t_{slipp}}. \quad (13)$$

Modeling of the combined slipping-slumping bed motion

This bed motion is expressed as a sum of these two flow patterns. The volume flux to be transported by the slumping flow pattern $\Phi_{V,Slump}$ is determined by

$$\Phi_{V,Slump} = \Phi_V - w_{d,slipp} \cdot \Gamma \cdot \frac{\pi \cdot D^2}{4}. \quad (14)$$

Where the filling ratio is denoted by Γ. is dThe differential equation developed by Saeman

$$\frac{d\ r_o}{d\ z^*} = \frac{3 \cdot \Phi_{V,Slump} \cdot \sin\upsilon}{4 \cdot \pi \cdot n^* \cdot \cos\upsilon \cdot (R^2 - r_o^2)^{3/2}} - \frac{\kappa}{\cos\upsilon} \quad (15)$$

is used for the slumping flow pattern. The slope of the bed $\frac{d\ r_o}{d\ z}$ is expressed for the combined flow pattern by

$$\frac{d\ r_o}{d\ z^*} = \frac{1}{w_{Sae}(r = r_o)}\frac{d\ r_o}{d\ t} \quad (16)$$

$$= \frac{w_{Sae}(r = r_o) + w_{dG}}{w_{Sae}(r = r_o)} \cdot \frac{d\ r_o}{d\ z}. \quad (17)$$

The velocity $w_{Sae}(r = r_o)$ is derived from the velocity equation of Saeman by evaluating the limit

$$\lim_{r\to r_o} n^* \cdot \sqrt{r^2 - r_o^2} \cdot \frac{\left(\kappa + \frac{d\ r_o}{d\ z^*} \cdot \cos\upsilon\right)}{\sin\upsilon} \cdot \frac{\pi}{\arccos\frac{r_o}{r}} = 2 \cdot r_o \cdot n^* \cdot \frac{\left(\kappa + \frac{d\ r_o}{d\ z^*} \cdot \cos\upsilon\right)}{\sin\upsilon}. \quad (18)$$

The rotational speed for the combined flow pattern is calculated from the discontinuously slipping model via

$$n^* = \frac{w_{d,slipp}}{\frac{dz}{d\upsilon}\Big|_{\upsilon=\arcsin\frac{R\cdot\sin\beta_Q}{rs}} \cdot \Delta\upsilon} \cdot (\upsilon_{r,u} - \upsilon_{r,l}). \quad (19)$$

Where $\upsilon_{r,u}$ is the upper and $\upsilon_{r,l}$ the lower angle of repose. The axial bed depth is shown for maize for various process conditions in figure 4. The experiments are in excellent agreement with the developed model. Additionally the measurements and model results of the residence time for maize via the the axial coordinate are shown in figure 5. The prediction of residence time is improved by the new model.

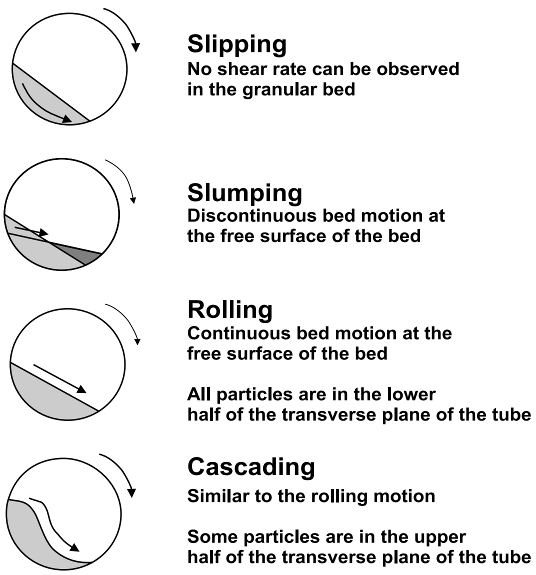

Figure 3: Basic flow patterns for granular bed motion in rotary kilns

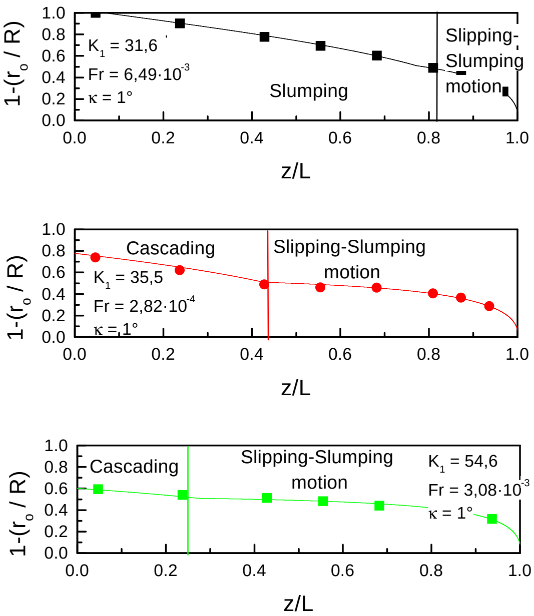

Figure 4: Measurements and model results of the bed depth for various process parameters

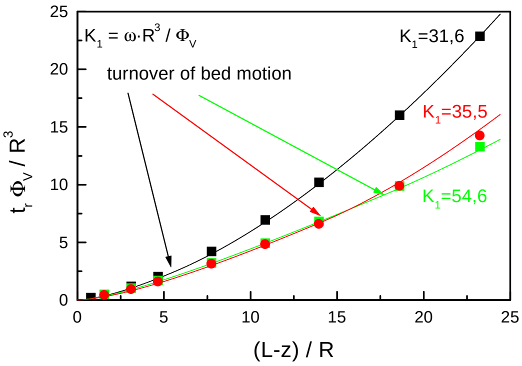

Figure 5: Measurements and results of the new transport model concerning the residence time t_r of maize along the axial coordinate

Conclusions

A brief description has been given dealing with different transport phenomena of the granular bed. A new flow type has been discovered. A model for discontinuous slipping and for the mixed slipping-slumping flow pattern has been developed. The model results are in very good agreement with the measurements.

References

[1] W. Heiligenstaedt. *Wärmetechnische Rechnungen für Industrieöfen*. Verlag Stahleisen m.b.H., Düsseldorf, 1966.

[2] H. Heinen, J.K. Brimacombe, and A.P. Watkinson. Experimental study of transverse bed motion in rotary kilns. *Metallurgical Transactions B*, 14B:191–205, 1983.

[3] W.C. Saeman. Passage of solids through rotary kilns. *Chem. Eng. Prog.*, 47:508–514, 1951.